

## METROLOGY OF VLSI CRITICAL ELEMENT SIZES

Yu. A. Novikov and A. V. Rakov

UDC 537.533

*Methods are surveyed for measuring the critical dimensions of VLSI components. The General Physics Institute of the Russian Academy of Sciences has developed a method that meets the requirements for metrological support up to the year 2010 as set out in the National Technology Roadmap for Semiconductors of the USA.*

In 1994, leading researchers in the USA published the National Technology Roadmap for Semiconductors, which reflects promising lines of development in microelectronics up to 2010 [1]. On these forecasts, the main material for the routine production of VLSI will be silicon. It is planned to use improved processes in microlithography by employing resist masks produced by ultraviolet or X-ray irradiation in order to produce appropriate topological patterns on the semiconductor wafers. Table 1 from [1] illustrates the main trends in VLSI manufacturing technology.

The table shows that the wafer diameter will increase in the fifteen-year period 1995–2010 from 200 to 400 mm, while the critical size (CS) of a microcircuit element (the minimum dimension of the element, e.g., the gate width in a field-effect transistor) from 0.35 to 0.07  $\mu\text{m}$  while retaining an error of measurement in the monitoring operation of 1% of the nominal value; there will also be tighter tolerances on the accuracy of matching between the topological patterns and a reduction in the pitch of the metal wiring from 1.0 to 0.3  $\mu\text{m}$  [1]. In [1] we find no data on particular technological approaches or on methods of monitoring the linear dimensions of the VLSI elements given in Table 1, and there is no discussion of ways of implementing the metrological requirements for the accuracy in these measurements.

This survey deals with ideas for measuring critical sizes of VLSI elements and ways of meeting the tight metrological specifications given in Table 1.

**Geometrical Models for VLSI Element Profiles.** The VLSI generated on a wafer gives the surface a microrelief as a consequence of chemical or plasmochemical etching in the corresponding layer via a lithographic resist mask. The components of current VLSI are produced by anisotropic etching, and this applies particularly to those planned for 2000–2010. The shape of such an element is usually close to that of a trapezium, and the side walls are nearly at  $90^\circ$  to the base. The higher the etching anisotropy, the closer the shape of the profile to a simple rectangle. Of course, the edges of the elements are rounded, but the idea of the element size usually relates to the geometrical model for the profile of trapezoidal or rectangular shape.

The term "critical size" widely used for VLSI elements corresponds to the size of the element whose profile is described by a rectangular model. However, in most practical cases a VLSI element has a shape to which the trapezoidal model should be applied (Fig. 1a). There are two critical sizes: the upper side ( $u_p$  or  $u_r$ ) and the lower side ( $h_p$  or  $h_r$ ) of the trapezium. The difference between these with a given depth for the relief (usually the thickness of the constructional layer) determines the etching anisotropy, which the technologist must know in order to set up the etching.

A particularly important task in producing VLSI is to monitor the sizes of the elements in the resist masks, which enables one to eliminate errors during the creation of such masks and to protect the wafer in all the technological operations. When one observes errors in the element sizes in the resist mask, they are readily eliminated, and a new layer of resist is deposited, on which lithography is performed, with the appropriate correction of the mask element sizes.

In order to measure submicron elements with an error of 1%, the method most suitable for realizing the Table 1 metrological requirements is at present scanning electron microscopy. We examine algorithms for measuring critical sizes by the use of the scanning electron microscope SEM.

TABLE 1. Development Prospects for Semiconductor Microelectronic Technology in the USA for the Period 1995-2010

Technological characteristics	Years					
	1995	1998	2001	2004	2007	2010
Wafer diameter, mm	200	200	300	300	400	400
Critical size CS, nm	350	250	180	130	100	70
Engineering tolerance on CS, nm	35	25	18	13	10	7
Error in measuring CS, nm	3.5	2.5	1.8	1.3	1.0	0.7
Tolerance on coincidence, nm	100	75	50	40	30	20
Coincidence error, nm	10	7.5	5	4	3	2
Metal wiring pitch, $\mu\text{m}$	1.0	0.8	0.55	0.35	0.3	0.3
Wiring pitch measurement error, nm	10	8	5.5	3.5	3.0	3.0

**SEM in Critical Size Metrology.** A fairly detailed survey has been given [2] of ideas on linear measurement with the SEM. The common basis is that the measurements are made only from the video signal VS recorded with slow secondary electrons SSE or in back-scattered electrons BSE on scanning the SEM probe over the relief element in a raster line. Figure 1b shows the scheme for the VS on recording the SSE; the differences between the proposed methods lie in the selection of the reference points on the VS curve, whose separations characterize the measurement element sizes: the distance between peaks ( $L_p$  or  $L_r$ ); distances between VS points lying at 40 or 50% of the signal level ( $L_H$  or  $B_H$ ); and distance between the points of intersection of a straight line passing through the average level of the background with the tangents to the flanks of the VS curve ( $B_p$  or  $B_r$ ). It is obvious that the distances between those points differ. Such deficiencies of these algorithms have been considered in [2].

After [2] had been prepared for publication, we obtained papers by the members of the National Institute of Standards and Technology NIST in the USA and of the National Physical Laboratory NPL in Britain that dealt with linear measurements on submicron components in the SEM. We consider those results as supplements to [2].

SEM transmitted electrons have been used [3] for the metrology of X-ray lithographic masks, which can be used in VLSI technology in the case of small critical sizes for the elements, e.g., less than 0.2  $\mu\text{m}$ . The experiments were performed with a reference SEM based on the AMRAY 1610 and with a S-400 SEM. The magnification was calibrated by means of the SRM-484 standard specimen. The transmitted electrons were recorded with a semiconductor detector. The signal was also simulated by the Monte Carlo method, which showed that the response curve is very sensitive to the slope of the element walls in the X-ray mask made of gold and lying on a membrane 2.5–3.5  $\mu\text{m}$  thick. The experiments showed that the main distortions in the VS curve are related to deviation from the vertical in the mask element walls, unevenness in the edges of these elements, and superposition of back-scattered electrons from the inclined wall on the transmitted electron signal.

It has been suggested [3] that the effective mask element width is equal to the segment between the points of intersection of the VS curve with the straight line passing through the 50% signal level. Table 2 gives the results from this experiment. The measurement error was about 10 nm [3] on passing from the mask element with the side wall inclined at 2° to the element in which the side wall inclination was 4° (angles reckoned from the normal to the surface), and this does not meet the metrological requirements in Table 1. That error was taken [3] as a systematic error.

A discussion of a possible universal algorithm for measuring VLSI element critical sizes [4] led to the conclusion that such an algorithm and the corresponding standard for the line width in SEM metrology requires exact models for electron beam interaction. It was considered [4] that at present one can make only exact linear measurements of the step in stepped submicron structures for which NIST has the standard SRM-2090 material, where the step between the elements is 0.2  $\mu\text{m}$  and has been determined and certified with nanometer accuracy.

The conclusion in [4] that one needs an exact model for beam interaction confirms that the existing models for VS formation in the SEM based on repeated elastic scattering and ionization caused by inelastic collisions are models that do not describe all the processes responsible for the VS. The inadequacy of those models has been confirmed by experiment [5].

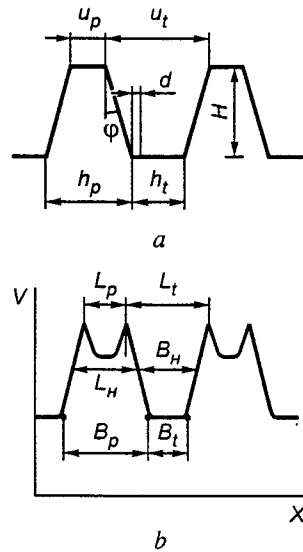


Fig. 1. Schemes for scanning a trapezoidal structure (a) and shape of video signal (b) showing measured and defining parameters.

TABLE 2. Resist Mask Element Sizes Measured in [3]

Nominal size, $\mu\text{m}$	Measured size, $\mu\text{m}$	Standard deviation <sup>1</sup> , $\mu\text{m}$
0.25	0.237	0.00015
0.35	0.363	0.0007
0.50	0.487	0.0028
0.75	0.740	0.0007

<sup>1</sup> This is the standard error of the mean evidently, which is not stated in [3], although it is stated that there were many measurements.

NPL publications [6–8] give VS simulation results for BSE in the experiments on phototemplate topology (chromium on glass). The distances between points on the VS curve for the back-scattered electrons at the 50% signal level are not dependent on the SEM probe diameter (when the probe size is less than the element size). The distance is taken as the size of the element at half height. The experimental sizes were compared with the calculated ones, which showed that there was a systematic error of about 10 nm [8], which does not satisfy the metrological specifications in Table 1. We consider that model VSs can be compared with observed ones if one can show that the experiments use photomasks having known sizes for the elements determined by alternative methods. However, it has been shown [8] that optical and electron-microscope measurements in the sub-micron range disagree widely. There are also papers on the metrology in the nanometer size range based on the scanning atomic force microscopy AFM [9, 10]. The AFM probe is the point of a needle, which provides information on the relief profile of nanometer size, but the height or depth of such an element should not exceed 100 nm, and the adjacent element should not be closer than 100 nm. These constraints limit the use of the AFM for monitoring contemporary VLSI, in which the heights or depths constitute from 0.1 to 1.0  $\mu\text{m}$  or more.

Also, when the height or depth is less than 100 nm, the signal curve in the AFM is dependent on the relief geometry and on the geometry of the point (shape of point spherical, parabolic, and so on). Therefore, as in SEM measurements, AFM ones require a standard structure having a known profile and certified element sizes, from which it is possible to determine the

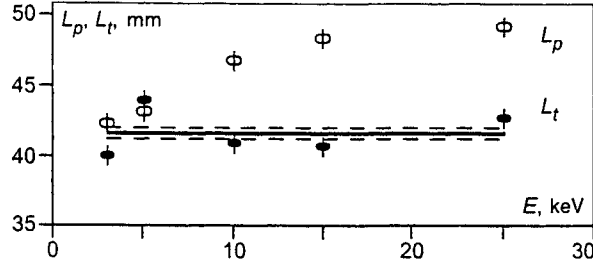


Fig. 2. Dependence of measured video signal parameters  $L_p$  and  $L_t$  on electron energy for the CamScan CS-44.

apparatus function. It has been shown [11] that it is possible to recover the profile without data loss when certain conditions specific to the AFM are met, but this is almost impossible in real experiments.

**Universal Algorithm for SEM Metrology of VLSI Element Critical Sizes.** The above results show that there is no single approach in the world practice to measuring VLSI element critical sizes. Detailed research has been done on the secondary electron emission physics of the solid surface at the General Physics Institute, Russian Academy of Sciences, which revealed a previously unknown effect of SSE emission from the surface states [5], which provided the universal algorithm for the purpose, and this is presented in detail in [12].

Briefly presented, this algorithm amounts to the following operations. First one calibrates the SEM (determines basic characteristics): the magnification  $M$ , the effective probe diameter  $d$ , and the correction parameter  $\delta$ , which indicates whether the SEM probe converges or diverges [12]. Then the recorded VS from the slow secondary electrons are used to measure two reference segments (Fig. 1) on scanning with the primary electron energy  $E > 10$  keV over the test element described by the model having a trapezoidal or rectangular profile (Fig. 1): the distances between the VS peaks ( $L_p$  and  $L_t$ ) and the distances between the points of intersection between the tangents to the left-hand and right-hand branches of the VS curve with the straight line at the average background level ( $B_p$  and  $B_t$ ). The subscripts  $p$  and  $t$  denote the shape of the element (step or groove respectively). Criteria have been given [12] for identifying the elements having profiles described by trapezoidal or rectangular forms.

The reference segments  $L$  and  $B$  are related to the sizes of the upper line  $u$  and lower line  $h$  of the relief element by

$$h_t = B_t/M + d, \quad (1)$$

$$u_t = (2L_t - B_t)/M - d \quad (2)$$

for the element as a groove with the trapezoidal profile and

$$h_p = B_p/M - d, \quad (3)$$

$$u_p = (2L_p - B_p)/M + d \quad (4)$$

for the element as a step with the trapezoidal profile.

For the element with a rectangular profile, we have

$$u_t = h_t = B_t/M + d = L_t/M - 2\delta \quad (\text{groove}) \quad (5)$$

and

$$u_p = h_p = B_p/M - d = L_p/M + 2\delta \quad (\text{step}) \quad (6)$$

That algorithm can be adapted to measuring a single critical size as determined by the mean line of the trapezoidal section. We add together (1) and (2) or (3) and (4) to get

TABLE 3. Measurements on  $L_r$ ,  $B_r$ ,  $L_p$ , and  $B_p$  for VS From Scanning Single Trapezoidal Steps and Grooves Having Nominal Sizes of 1.0 and 1.2  $\mu\text{m}$  for Various SEM Probe Diameters (Focusing and Defocusing)

Size, $\mu\text{m}$	Probe diameter, nm	Step		Groove	
		$L_p$ , mm	$B_p$ , mm	$L_r$ , mm	$B_r$ , mm
1.0	114 $\pm$ 6	61.3 $\pm$ 0.7	73.0 $\pm$ 1.1	55.9 $\pm$ 0.9	44.9 $\pm$ 1.0
	397 $\pm$ 16	59.1 $\pm$ 1.4	88.0 $\pm$ 1.8	59.2 $\pm$ 1.2	29.8 $\pm$ 1.1
1.2	114 $\pm$ 6	75.8 $\pm$ 0.9	87.1 $\pm$ 0.9	71.4 $\pm$ 0.7	61.1 $\pm$ 0.9
	397 $\pm$ 16	73.1 $\pm$ 1.3	100.2 $\pm$ 1.2	75.7 $\pm$ 1.8	44.5 $\pm$ 1.6

TABLE 4. Measured Parameters of Single Steps and Grooves Having Nominal Sizes of 1.0 and 1.2  $\mu\text{m}$  for Two SEM Models, Various Electron Energies, and Various Probe Diameters

Size, $\mu\text{m}$	SEM			Step		Groove	
	Model	$E$ , keV,	$d \pm \Delta d$ , nm	$u \pm \Delta u$ , nm	$h \pm \Delta h$ , nm	$u \pm \Delta u$ , nm	$h \pm \Delta h$ , nm
1.0	SEM 515	10	77 $\pm$ 2	940 $\pm$ 20	1050 $\pm$ 30	1000 $\pm$ 30	870 $\pm$ 20
		16	75 $\pm$ 2	961 $\pm$ 6	1090 $\pm$ 7	1015 $\pm$ 9	911 $\pm$ 6
	CamScan S-4	15	83 $\pm$ 3	1019 $\pm$ 14	1141 $\pm$ 14	1020 $\pm$ 15	900 $\pm$ 9
		25	71 $\pm$ 16	970 $\pm$ 40	1100 $\pm$ 50	1030 $\pm$ 40	840 $\pm$ 30
1.2	SEM 515	10	77 $\pm$ 2	1150 $\pm$ 30	1260 $\pm$ 30	1290 $\pm$ 30	1160 $\pm$ 30
		16	75 $\pm$ 2	1163 $\pm$ 7	1331 $\pm$ 8	1325 $\pm$ 8	1216 $\pm$ 7
	CamScan S-4	15	83 $\pm$ 3	1233 $\pm$ 16	1338 $\pm$ 16	1306 $\pm$ 18	1199 $\pm$ 13
		25	71 $\pm$ 16	1230 $\pm$ 50	1330 $\pm$ 50	1290 $\pm$ 50	1170 $\pm$ 40
			114 $\pm$ 6	1230 $\pm$ 40	1400 $\pm$ 30	1300 $\pm$ 40	1170 $\pm$ 20

$$\frac{L_t}{M} = \frac{u_t + h_t}{2}, \quad (7)$$

$$\frac{L_p}{M} = \frac{u_p + h_p}{2}. \quad (8)$$

Formulas (7) and (8) differ from (1)–(4) in not containing  $d$  (probe spot size), i.e., the distances between VS maxima are not dependent on the SEM probe focusing.

This feature of the modified algorithm for measuring the mean line of a trapezoidal section in a VLSI element enables one to automate the SEM measurement because it is then not necessary to automate the probe focusing. The algorithm with (7) and (8) can be recommended for monitoring microlithography if the technologist already knows the anisotropy of the local plasmochemical etching.

An experimental test has been performed [13] on that algorithm for slot structures in the form of rectangular grooves, where it was shown that groove widths from 90 to 500 nm give an average error in (5) of not more than 1% of the size. In [14–16], a check was made on (1)–(4) in measuring the sizes of trapezoidal-profile elements by means of a special test structure.

The reference segments  $L_p$  and  $L_r$  characterize the mean line in a trapezoidal element and should be identical for various electron energies  $E$  and should not be dependent on the size of the probe spot. Table 3 gives measurements on  $L_p$ ,  $L_r$ ,  $B_p$ , and

TABLE 5. Measured Values of Mean Line  $(u + h)/2$  in Trapezoidal Steps and Grooves Having Nominal Size  $0.55 \mu\text{m}$  and Steps in Distance Between Equivalent Maxima  $L_p$  and  $L_r$ , and Boundaries of the Base of the Video Signal  $B_p$  and  $B_r$  in a Resist Step Structure (Resist Ridges on Silicon and Grooves in a Resist Film on Silicon)

Structure type	Step number	$(u + h)/2$ , nm		Step, nm	
		Groove	Ridge	$t_L$	$t_B$
Ridge on silicon	1	711±16	293±9	1004±18	1080±21
	2	—	227±6	—	—
Groove in resist	1	838±21	231±8	1069±22	982±19
	2	736±20	300±13	1036±24	1091±23

TABLE 6. Values of Upper and Lower Ends of Trapezoidal Ridges and Grooves Having Nominal Dimension  $0.55 \mu\text{m}$  in a Resist Step Structure (Resist Ridges on Silicon and Grooves in a Resist Film on Silicon)

Structure type	Element number	Groove		Ridge	
		$h_r$ , $\mu\text{m}$	$u_r$ , $\mu\text{m}$	$h_p$ , $\mu\text{m}$	$u_p$ , $\mu\text{m}$
Ridge on silicon	1	0.56	0.86	0.52	0.07
	2	—	—	0.38	0.07
Groove in resist	1	0.59	1.09	0.39	0.07
	2	0.57	0.90	0.52	0.08

$B_r$  on scanning the same elements in the same area but with various probe diameters. We see that  $L_p$  and  $L_r$  are constant within two standard deviations, while  $B_p$  and  $B_r$  vary considerably, as implied by (1), (3), (7), and (8).

Figure 2 shows the dependence of  $L_p$  and  $L_r$  on  $E$  in the range from 3 to 25 keV for single steps and grooves having nominal size  $1.0 \mu\text{m}$ . The VS curves were recorded at the fixed magnification  $M$ . We see that  $L_r$  is independent of  $E$  within the error range; only one point at  $E = 5$  keV lies outside that range. The picture is different for the step, and there is a monotone decrease in  $L_p$  as  $E$  falls, particularly for  $E < 10$  keV. No explanation exists for the difference in behavior of  $L_p$  and  $L_r$ , but one may conclude that (7) and (8) apply for  $E > 10$  keV.

It is confirmed that the measured sizes of trapezoidal profile elements are independent of the electron energy for  $E > 10$  keV by the determinations of the upper and lower lines bounding single steps and grooves having nominal dimensions of 1 and  $1.2 \mu\text{m}$  for the range  $E = 10\text{--}25$  keV.

Table 4 gives these data. Within the error limits (1–3% of the measured value), the results agree within the range in  $E$  for the measurements with two SEM models.

The [2] NIST measurements on a given element with variable  $E$  (1.5 to 30 keV) showed that the size was dependent on  $E$ , which indicates that the algorithm was incorrect.

Resist mask experiments showed that a given probe current and  $E > 10$  keV produced video signal noise with slow secondary electrons from the resist masks at such a high level that it was almost impossible to determine the positions of the maxima. To reduce the noise contribution, one can sum the VS by lines, and as the noise is uncorrelated, the contribution to the summed VS curve is reduced. That reduces the noise contribution by a substantial factor, so it is possible to determine the characteristic features (peaks) on the summed VS curve.

An MK-51 photoresist mask  $1.2 \mu\text{m}$  thick on silicon constituted two types of the stepped structures: slot-type grooves in the resist film and resist ridges on the silicon. The given nominal size of each element in these structures was  $0.55 \mu\text{m}$ , while the structure step was  $1.1 \mu\text{m}$ . The edge elements in the stepped structures were not measured. The values of  $L_p$ ,  $L_r$ ,  $B_p$ , and  $B_r$

were determined from the VS curve obtained by summing ten single video signals. The mean lines of the step and groove (trapezoidal) were calculated from (7) and (8).

Table 5 gives measurements on the mean lines for trapezoidal ridges and grooves in the resist mask and the step in the structure (sum of the mean lines of groove and ridge). The mean step in the structure was  $t = 1.04 \mu\text{m}$ ; the standard deviation was  $\sigma = 0.04 \mu\text{m}$ . This reproduces quite closely twice the value of the nominal mask element size. Also,  $\sigma$ , here characterizes not the error of measurement but the performance in developing the photoresist mask.

Table 5 shows that the sizes of the mean lines for the ridges and grooves in the mask vary widely:  $0.23\text{--}0.30 \mu\text{m}$  for ridges and  $0.71\text{--}0.84 \mu\text{m}$  for the grooves. These results show that the nominal mask element size does not correspond to the mean the profile line. To establish what corresponds to the nominal element size, we determine the sizes of the upper and lower ends of the groove and the ridge (Table 6), which showed that the nominal size in fact characterizes the size at the level of the silicon surface (lower end). There are two ridges whose widths are very different from those of the others, which indicates deficiencies in the preparation of this mask, although those deviations have only a slight effect on the step size.

These data show that critical-size metrology for VLSI elements in the submicron range can be handled by the method developed at the General Physics Institute for elements having closely trapezoidal or rectangular profiles. The proposed universal algorithm has been tested on various SEM models. A recommendation is made on using it with two reference segments on the video signal curve in order to monitor structures obtained in fully established technologies. The VLSI elements made in a fully established process can be monitored from a single critical size: the mean profile length.

One can use (1)–(8) in the universal algorithm for measuring the critical sizes of VLSI elements on an SEM at an electron energy  $E > 10 \text{ keV}$ , and it is found that the error in measuring such sizes is dependent on the errors in determining the major SEM characteristics: magnification  $M$  and effective probe diameter  $d$ . Formulas are given for selecting conditions under which one best meets the metrological specifications given in Table 1.

## REFERENCES

1. *The National Technology Roadmap of Semiconductors*, SIA, San Jose, California, USA (1994).
2. Yu. A. Novikov and A. V. Rakov, *Mikroelektronika*, **25**, No. 6, 417 (1996).
3. M. T. Postek et al., *J. Res. Nat. Inst. Stand. Technol.*, **98**, No. 4, 415 (1993).
4. M. T. Postek, *J. Res. Nat. Inst. Stand. Technol.*, **99**, No. 5, 641 (1994).
5. Yu. A. Novikov and A. V. Rakov, *J. Moscow Phys. Soc.*, **5**, No. 5, 229 (1995).
6. J. W. Nunn and N. P. Turner, *Scanning*, **11**, 213 (1989).
7. J. W. Nunn, *Scanning*, **12**, 257 (1990).
8. J. W. Nunn, *Scanning*, **17**, 296 (1995).
9. T. H. McWaid et al., *Nanotechnology*, **5**, 33 (1994).
10. M. Nagase et al., *Jpn. J. Appl. Phys.*, **34**, No. 6B, 3382 (1995).
11. A. A. Bukharev et al., *Mikroelektronika*, **26**, No. 3, 163 (1997).
12. Yu. A. Novikov and A. V. Rakov, *Mikroelektronika*, **25**, No. 6, 426 (1996).
13. V. A. Danilov, Yu. A. Novikov, and A. V. Rakov, *Izmer. Tekhn.*, No. 4, 23 (1995).
14. Yu. A. Novikov et al., *Elektron. Promyshlennost'*, No. 3, 50 (1995).
15. Yu. A. Novikov et al., *Preprint GPI RAS*, No. 18, 12 (1995).
16. Yu. A. Novikov and A. V. Rakov, *Preprint GPI RAS*, No. 3, 9 (1996).